Catalysis Letters, Vol. 115, Nos. 3–4, June 2007 (© 2007)
DOI: 10.1007/s10562-007-9076-y

Metallic monolith supported $LaMnO_3$ perovskite-based catalysts in methane combustion

Barbara Kucharczyk and Włodzimierz Tylus*

Institute of Inorganic Technology and Mineral Fertilizers, Wrocław University of Technology, Wybrzeże St. Wyspiańskiego 27, Wrocław 50-370, Poland

Received 3 January 2007; accepted 28 February 2007

Metallic monolith supported $LaMnO_3$ perovskite-based catalysts are characterized by a high activity in methane combustion (95.5% conversion at 745 °C) and by a high thermal resistance. The activity of the catalysts depends on the duration and temperature of $LaMnO_3$ calcination. The same relation holds for the chemical composition of the catalyst surfaces when they are determined by the XPS method. The shortening of the time of $LaMnO_3$ perovskite calcination from 12.5 h to 8 h (700 °C) reduces the conversion of methane over a fresh catalyst. This is attributable to the lower amount of manganese (Mn:La = 0.48) on the surface of this catalyst compared to the catalyst whose perovskite was calcined for 12.5 h (Mn:La = 1.8). The extension of calcination time from 8 h to 12.5 h (at 700 °C) brings about a decrease in the specific surface area (SSA) from about 13.7 m^2/g to 9.4 m^2/g. After approximately 6 h on stream, the activities of the two catalysts become comparable. Aging of the catalyst with an $LaMnO_3$ active layer at 920 °C for 24 h reduces methane combustion to 82.5% (at 745 °C). The aging process changes the catalyst surface, where Al and C content increases and the Mn:La ratio decreases. The activity of the monolithic $LaMnO_3$ catalyst rises with the increase in the amount of the active layer from 11.5% to 17.8%. Methane conversion is greater over catalysts with an $LaMnO_3$ than with an $LaCoO_3$ active layer, but the $LaMnO_3$ catalysts show a lower resistance to thermal shocks.

KEY WORDS: monolithic catalysts; perovskites; methane combustion; XPS.

1. Introduction

Perovskite oxides of the generalized formula ABO_3 show good catalytic properties in methane combustion and a high thermal resistance [1–5]. Catalytic activity is ascribed to the metal in position B, while the ion in position A is responsible for the thermal resistance of the catalyst [3,4]. Such catalysts apply to catalytic combustion processes where not a high activity at low temperature but a high thermal resistance and durability of the catalyst is needed [5,6]. High activity in methane combustion is a characteristic feature of perovskites with lanthanum as metal A ($LaBO_3$), and Co, Mn, Fe, Cr or Ni as metal B [4,7]. The catalytic activity of these perovskites decreases in the following order: $LaCoO_3 LaMnO_3 LaFeO_3$ [2,5–9]. The use of Nd as metal A has also been reported ($NdCoO_3$) [10,11]. A large group of catalysts that are active in methane combustion includes perovskites of type $AFeO_3$ with La, Nd or Sm as metal A [11]. An important factor affecting the performance of perovskite catalysts is the method of preparation, which should provide a high specific area, homogeneity and catalytic activity [4,5]. In the preparation procedure, the temperature of perovskite calcination plays an important part, as it is responsible for the sizes of the perovskite crystals and surface area. The comparatively low calcination temperature, ranging between 700 and 750 °C, is an obstacle to achieving a high thermal stability of the catalyst [12].

Methane combustion is also carried out over perovskites where the metal in position A and/or that in position B has partly been replaced with another metal. In this way a large group has been formed of active oxides described by the generalized formula $A_{1-x}A_xB_{1-y}B_yO_3$ [1,2, 13–15]. The substitution of the metal in position A with lower-valency cations accounts for a variations in the oxidation state of the metal in position B or to the formation of oxygen vacancies and lattice defects [2,9,13].

Perovskite catalysts are used predominantly in the form of cylinders and rings, though use is also made of honeycomb monoliths for methane combustion. Initially, honeycomb monoliths were prepared by extrusion of plastic pastes composed of perovskite powders with the addition of binders, acid peptizers and some surfactants [16]. Attempts have also been made to deposit the active phase of the perovskites onto a ceramic monolithic support, generally made of cordierite and frequently washcoated with γ-Al_2O_3 [3,5]. Compared to conventional fixed-bed catalysts, monolith-supported catalysts have some unquestionable advantages. The pressure drop remains very low for high-cell density monoliths, and the desired extent of conversion is obtained with a smaller amount of the perovskite [1,15].

*To whom correspondence should be addressed.
E-mail: tylus@pwr.wroc.pl

The aim of the study reported on in this paper was to examine the physicochemical properties and activities of metallic monolithic $LaMnO_3$ and $LaCoO_3$ perovskite-based catalysts. The activities of the catalysts were compared with the activity of a monolithic catalyst with $LaCoO_3$ as the active layer, prepared via the same method. As is the case with the three-way catalysts that are mounted in cars, the metallic monolith used in our study was made of a washcoated heat-resisting FeCrAl foil.The replacement of the ceramic monolith with a metallic one seemed advisable due to the following advantages: a larger free cross-section, a higher thermal resistance, and a greater heat conductivity, which provides a quicker heating of the monolithic support [17].

2. Experimental

2.1. Catalysts preparation

Monolithic catalysts were prepared on a support made of heat-resisting FeCr20Al5 foils (00H20J5), smooth and crimped, cylindrically wound (70 mm in length and 26 mm in diameter, average weight 22.15 g), with a honeycomb cross-section. The channels of the monolith (112 per square centimetre) were triangular in shape (the side of the triangle being 1.4 mm long). Each foil was coated with an 84.8% Al_2O_3 , 14.4% TiO_2 and 0.8% La_2O_3 washcoat, using the sol–gel method. The sol was prepared by mixing calculated amounts of $Al(OH)_3$ (obtained by the hydrolysis of aluminium isopropoxide (Aldrich)), TiO_2 (Aldrich) and $La(NO_3)_3 \cdot 6H_2O$ (Fluka). Thereafter the sol was treated with a buffer solution until the pH of 7.5 was achieved, and stirred at a rate of 500 rpm at room temperature for 2 h to obtain a stable sol. The monolithic support was immersed in the sol, dried at room temperature for 4 h and thereafter at 110 °C for 3 h, and then calcined at 400 °C for 3 h. The amount of the washcoat totalled 2 wt.% with respect to the support mass. Oxides of perovskite type, $LaMnO_3$ or $LaCoO_3$, were used as active phases. Perovskites were obtained by drying at 110 °C an aqueous solution of $La(NO_3)_3 \cdot 6H_2O$ (Fluka) and $Mn(NO_3)_2 \cdot 4H_2O$ (Merck) or $Co(NO_3)_2 \cdot 6H_2O$ (Fluka), and calcined at 700 °C for 8 h, 11 h and 12.5 h or at 750 °C for 6 h (heating ramp 10 °C/min). Upon calcination, the perovskites were ground in a mortar and sieved (mesh diameter, 0.07 mm). The perovskite powders are characterized in table 1.

The active layer was deposited by dipping the support into a suspension obtained by mixing the perovskite powder and citric acid of a concentration of 2.8 mol/dm^3 at a weight ratio of 1:3. The catalysts varied in the amount of the active layer; the mass of the perovskite powder ranged between 12 and 23 wt.% of the mass of the monolithic support (table 1). The catalysts were calcined in air at 500 °C for 3 h (heating ramp 2 °C/min). Upon deposition of the active layer, the average weight of the catalysts used in activity tests amounted to 25.7 g when the perovskite was calcined at 700 °C for 8, 11 or 12.5 h. The weight of the other catalysts varied from 25.14 to 27.62 g, depending on the amount of the active layer on the support (table 1).

2.2. Catalysts characterization

Phase composition was examined by the X-ray powder diffraction (XRD) method, using a Philips Materials Research Diffractometer. Measurements were carried out in the parallel beam optics. In the course of measurements, the active layer was illuminated at a constant angle ($\omega = 5°$), the scan being 2Θ.

Additionally the surface of the sample was examined by scanning electron microscopy (SEM), using a JSM 6800LV instrument (made by Jeol), equipped with an ISIS 300 Oxford microanalysis system (EDS).

The surface composition of the catalysts was analyzed by X-ray photoelectron spectroscopy (XPS), using a SPECS UHV system equipped with a PHOIBOS 100 spectrometer and SpecLab software. The X-ray source was generated with an Mg anode operating at 100W (survey scan) and 200–300 W (high resolution spectra). The analyzer mode was set at constant pass energy (30 eV survey scan and 5 eV narrow scan). Sample charging was compensated, using an electron flood at 0.5 mA current and 0.1 eV energy. The detection angle was normal to the surface.

BET specific surface areas (SSA) were calculated from the nitrogen sorption isotherms measured by the static volumetric method at liquid nitrogen temperature with an Autosorb-1C apparatus from Quantachrome Instruments. Adsorption measurements were carried out with outgassed (at 150 °C) catalyst samples until the pressure rise limit was equal to, or lower than, 20 μmHg/min. Making use of the N_2 sorption isotherm, the values of microporosity were established according to the de Boer method. Pore distribution values were determined from the desorption branch, using the BJH (Barrett, Joyner, Halenda) method.

Investigations were also carried out into the resistance of the catalysts to thermal shocks. In an oven of special design, the samples were subjected to 4000 cycles of heating up to 1000 °C and subsequent cooling down to room temperature. Each cycle took 30 s and included the introduction of the sample into the oven at 1000 °C, removal of the sample and cooling down to room temperature. The change in the sample mass (after a certain number of cycles), compared to the initial mass of the washcoated and perovskite-coated monolith, was regarded as a measure of resistance to thermal shock.

2.3. Catalytic activity measurements

Catalytic activity was tested in the combustion of 1% methane in air over the monolithic catalysts, using a

Table 1
Preparation parameters and characterization of the perovskite powders

Composition of perovskites	Amount of perovskites in catalysts (wt.%)	Calcination temperature (°C)	Calcination time (h)	Mean pore diameter, (nm)	SSA (m^2/g)	Apparent activation energy (kJ/mol)
$LaMnO_3$	14.6	700	8	37.6	13.74	86.3
$LaMnO_3$	14.0	700	11	38.0	12.89	72.6
$LaMnO_3$	13.8	700	12.5	37.5	9.45	73.2
$LaMnO_3$	11.5	750	6	8.5; 35	8.58	87.3
$LaMnO_3$	17.8	750	6	–	8.58	87.3
$LaCoO_3$	14.0	750	6	16.4–23.9	5.69	97.1
$LaCoO_3$	22.7	750	6	–	5.69	97.1

throughflow reactor (i.d., 26 mm; length, 400 mm) placed in a heater with a programmed temperature increment (heating ramp 3 °C/min). Total gas hourly space velocity (GHSV) was fixed at 5800 h^{-1} (total flow rate 202 dm^3/h). The conversion of methane was measured over the temperature range of 350–780 °C. The inlet and outlet methane concentrations were analyzed with a Sniffer analyzer (Bacharach) (measuring range 1–10,000 ppm). Monoxor II (measuring range 1–1999 ppm) and Nonoxor II analyzers (Bacharach) (measuring range 1–1999 ppm) were used to measure the concentrations of CO and NO_x, respectively. The accuracy of the analyzers used in this study was ± 5% of the measured value.

Following the completion of the catalytic activity tests, the catalysts were aged in air by heating them in an oven at 920 °C or 1000 °C for 24 h, removing them after that period, and cooling them quickly to room temperature.

3. Results and discussion

3.1. X-ray diffraction

The XRD patterns of catalyst surfaces with $LaMnO_3$ active layers for perovskites calcined at 700 °C for 8 h (fresh catalyst) and 12.5 h (fresh, after 20 h on stream and aged at 1000 °C for 24 h) are included in figure 1. The XRD pattern in figure 1a shows that after 8 h of calcination the $LaMnO_3$ perovskite is the main phase in the active layer. However, the presence of small La_2O_3 peaks suggests an incomplete formation of the perovskite. The XRD pattern of the catalyst with the perovskite calcined for 12.5 h (figure 1b) displays the presence of a single $LaMnO_3$ phase in the active layer. The spectra of both catalysts show peaks associated with the monolithic support (Fe–Cr). The spectrum of the $LaMnO_3$ catalyst after 20 h on stream at 750 °C exhibits small Al_2O_3 peaks, which become clear and distinct after 24 h aging at 1000 °C (figure 1c and d, respectively). This is an indication that at high temperature Al_2O_3 segregates to the surface.

3.2. XPS measurements

The XPS spectra of lanthanum are difficult to interpret because of the presence of satellite peaks. For lanthanum, the closed-shell La^{+3} ion shows its La $3d_{5/2}$ and La $3d_{3/2}$ peaks split by approximately 4 eV into two components, which has been assigned to the transfer of an oxygen-centred electron to the empty 4f shell accompanying the ionization process. These energy loss peaks appearing on the high energy side of the 3d5/2 peaks in figures 2 and 3 are referred to as satellite peaks. Besides, the satellite peak intensity in the La 3d doublet

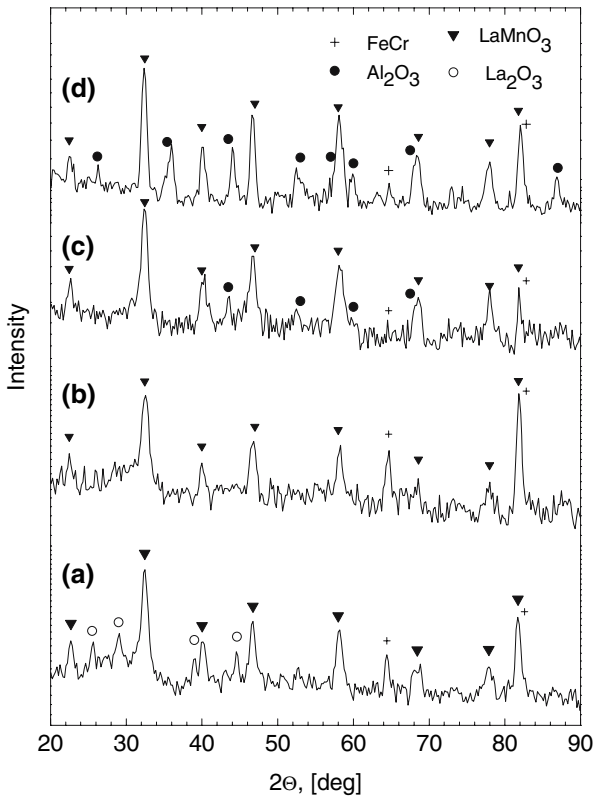

Figure 1. XRD patterns of monolithic $LaMnO_3$ fresh catalyst after calcination of perovskite powders at 700 °C for 8 h (a) and 12.5 h (b); catalyst after 20 h on stream (c), catalyst aged at 1000 °C for 24 h (d). In figure 1c and d, perovskite powders were calcined for 12.5 h.

varies with temperature [18]. Figures 2 and 3 show the La $3d_{5/2}$ spectra of the catalysts with $LaMnO_3$ perovskites calcined at 700 °C for 8 h and 12.5 h (fresh, after 20 h on stream, and aged at 1000 °C for 24 h). In both figures, the spectra are compared with the spectrum of pure La_2O_3.

With the catalysts calcined at 700 °C for 12.5 h, the shapes of the La $3d_{5/2}$ peaks (figure 2b, c and d) are, after height normalization, very similar: the main peak and its satellite peak are equally separated; the satellite peak has the same position, 837.787 eV; almost the same position is that of the main peak, 834.1 ± 0.1 eV; and similar are the FWHM values: 6.44, 6.22 and 6.21 eV, respectively. The slightly higher FWHM value for the fresh sample is likely to be linked with the presence of the carbonate groups which decomposed both after the run and at elevated temperature. At the same time, the spectra are distinctly shifted towards lower binding energies by 0.7 eV as compared to La_2O_3 . The results show that the catalyst is stable, resistant to thermal shocks, and has a totally perovskite structure. XRD analyses, which have revealed an $LaMnO_3$ structure alone, substantiate this finding.

The La 3d spectrum of the fresh catalysts after 8-h calcination of the perovskite differed notably from that of the catalyst calcined for 12.5 h. The spectrum confirmed the presence not only of La_2O_3 (substantiated by XRD analyses) but also of the metalorganic fraction coming from the reaction of La_2O_3 with citric acid which is used when depositing the perovskite suspension onto the metallic surface of the support. After 20 h on the run, no metalorganic fraction was present on the catalyst surface. However, the proportion of La_2O_3 to $LaMnO_3$ was still considerable. Based on the deconvolution of the La $3d_{5/2}$ peaks (figure 3c), the $La_{oxide} : La_{perovskite}$ ratio was assessed at 0.25. Following a quantitative analysis of La and Mn (table 2), the $La_{oxide} : La_{perovskite}$ ratio was set at 0.4. It is worth noting that, besides the dominant perovskite structure, XRD analysis revealed only trace amounts of La_2O_3 . There is, however, no inconsistency between the results of XRD and those of XPS. Being very sensitive with respect to surface issues, the latter technique suggests a considerable La_2O_3 -enrichment of the catalyst surface resulting from the segregation of lanthanum to the surface during thermal processing of the catalyst. After 24-h ageing at 1000 °C, the composition of the catalyst surface approached the bulk composition, i.e. La:Mn = 1, and the assessed binding energies of La $3d_{5/2}$ electrons, amounting to 834.1 eV and 837.77 eV for the main peak and the satellite peak, respectively, are characteristic for the $LaMnO_3$ perovskite. The atom composition of the catalyst surfaces is summarized in table 2.

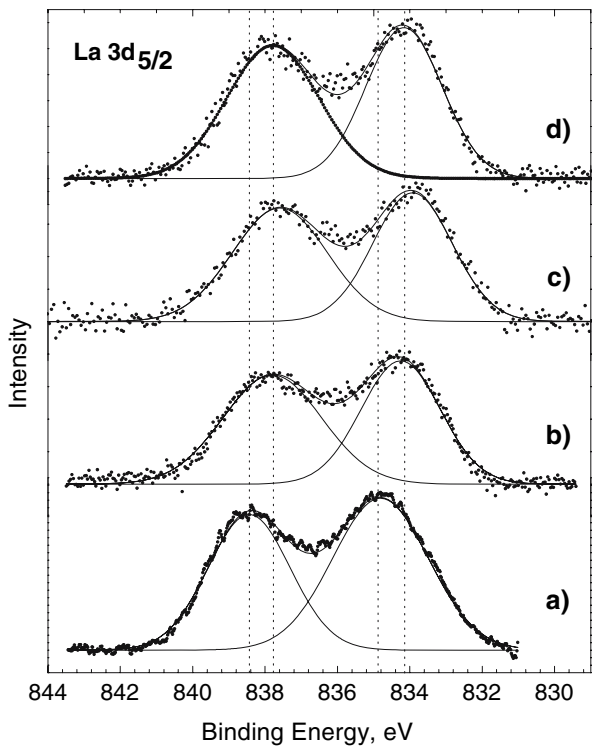

Figure 2. XPS spectra of La 3d in: (a) La_2O_3 ; (b) fresh $LaMnO_3$ perovskite calcined at 700 °C for 12.5 h; (c) the same catalyst after 20 h on stream; (d) the same catalyst after aging at 1000 °C for 24 h.

Mn 2p XPS spectra have been of limited value due to difficulties in differentiating among the contributions of Mn^{+2}, Mn^{+3}, and Mn^{+4} to the spectra of most solid Mn phases [19–21]. The difficulties are twofold. First, the peak maxima for the three ions are separated by less than two eV, making it difficult to resolve the separate contributions using most instruments; even partial resolution requires peak widths to be less than 1.4 eV the full width at half of maximum (FWHM). Second, Mn^{+2}, Mn^{+3} and Mn^{+4} generally assume high spin states in oxides [22], and in high spin states the 2p XPS spectrum of each is composed of numerous peaks (multiplets) that result in unusually broad, compound Mn (2p3/2) spectra. That is why the interpretation of the spectra obtained can only be of an illustrative nature. Figures 4 and 5 show the Mn $2p_{3/2}$ spectra of the catalysts with perovskites calcined for 8 h or 12.5 h (fresh, after 20 h on stream, and aged at 1000 °C). The spectra were compared with those of MnO_2, Mn_2O_3 and MnO in order to illustrate the potentiality of Mn occurrence at various stages of oxidation. A significant difference has been observed with fresh samples.

The peak of the catalyst after 8 h of calcination is notably broader, with an FWHM value of 3.9 eV compared to the 3.0 eV value of the catalyst after 12.5 h of calcination. The broadening of the peak by about 0.9 eV was towards higher energies. This implies the presence of non-oxide Mn compounds, probably linked with the occurrence of manganese citrate which has not been completely decomposed during 5-h calcination of the catalyst at 500 °C.

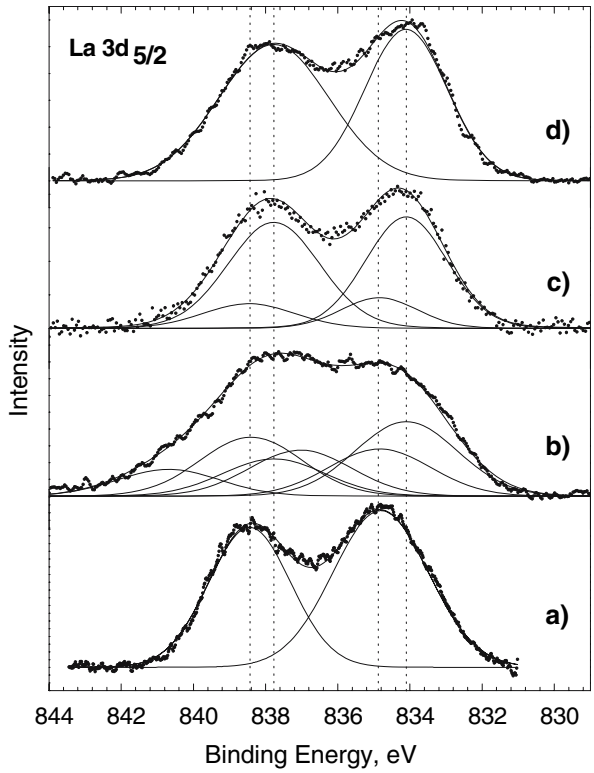

Figure 3. XPS spectra of La 3d in: (a) La_2O_3 ; (b) fresh $LaMnO_3$ perovskite calcined at 700 °C for 8 h; (c) the same catalyst after 20 h on stream; (d) the same catalyst after aging at 1000 °C for 24 h.

The Mn $2p_{3/2}$ spectrum of the catalyst with a perovskite calcined for 12.5 h (figure 4d) resembles (in terms of the position of the peak maximum and the FWHM value) the spectrum for MnO_2, which suggests the dominance of Mn^{+4} on the surface of the fresh catalyst. The XPS spectra recorded after 20 h on stream are visibly shifted towards lower energies, and this implies the occurrence of Mn^{+3}, or even Mn^{+2}. The broader top of the peak at 12.5-h calcination (figure 4e), as compared to that at 8-h calcination (figure 5e), may be indicative of a greater proportion of Mn^{+3} (and Mn^{+2}) forms on the surface of this catalyst. It is also worthy to note that the surface of this catalyst is much richer in manganese than the surface of the catalyst after 8-h calcination of the perovskite. The Mn:La ratios for fresh catalysts amounted to 1.8 and 0.5, respectively, and rose to 2.5 and 0.6, respectively, after 20 h on stream as a result of Mn segregation to the surface (table 2). After aging of the catalyst at 1000 °C, the shapes of both peaks, their positions and FWHM values became identical, which suggests a very similar structure of manganese fixation in the two catalysts. The difference in the Mn:La ratios between the catalysts decreased, so they amounted to 1.7 and 0.9, respectively, after aging (table 2).

After deposition of the perovskite layer, aluminium oxide that acted as the washcoat was not detected by XPS examinations on the surface of the catalyst – either after 8 h or 12.5 h of calcination at 500 °C. However, while the catalyst was on stream, but primarily after aging at 1000 °C, segregation to the surface was observed. For the catalyst calcined for 8 h, relevant Al:Mn and Al:La atom ratios amounted to 0.08 and 0.2, respectively, after 20 h on stream; after aging they were 0.9 and 1.5, respectively. For the catalyst calcined for 12.5 h, the said atom ratios totalled 0.13 and 0.08 after the run, respectively, and 0.9 and 0.85 after aging, respectively (table 2). The progressing segregation of Al to the catalyst surface at elevated temperatures may have contributed to the formation of new aluminium compounds: $LaAlO_3$, $La_2O_3 \cdot 11Al_2O_3$ or $MnAl_2O_4$. However, according to the available literature, there is little probability that these compounds will form below 1000 °C, since their formation has been observed at 1200 °C [22–26]. This finding was confirmed by our XPS and XRD examinations. Figure 6 shows the XPS Al 2p spectra for some surfaces of choice. The BE of Al 2p on the surface of a fresh washcoat calcined at 400 °C amounts to 74.1 eV (figure 6a) and is characteristic for γ-Al_2O_3 ; the comparatively high FWHM value, 2.33 eV, indicates that, besides the gamma form, there are also hydrated forms, e.g. $AlOOH \cdot H_2O$. The rise in calcination temperature brought about a shift of the peak maximum towards lower binding energies; after 1000 °C, the BE of Al 2p was only 73.9 eV, and the FWHM value fell to 1.83 eV (figure 6d). The drop in the

Table 2
Surface composition of $LaMnO_3$ perovskite catalysts calcinated at 700 °C for 12.5 and 8 h

Composition of active phase	Atom concentration (at. %)				
	La	Mn	O	Al	C
$LaMnO_3$ calcinated for12.5 h					
Fresh	7.11	12.85	52.57	0	27.48
After 20 h on stream	5.53	13.88	47.29	1.14	32.16
After aging	4.1	7.0	36.5	6.2	46.2
$LaMnO_3$ calcinated for 8 h					
Fresh	10.23	4.87	54.14	0	30.76
After 20 h on stream	10.61	6.42	46.38	0.85	35.73
After aging	7.3	6.8	45.3	6.2	34.4

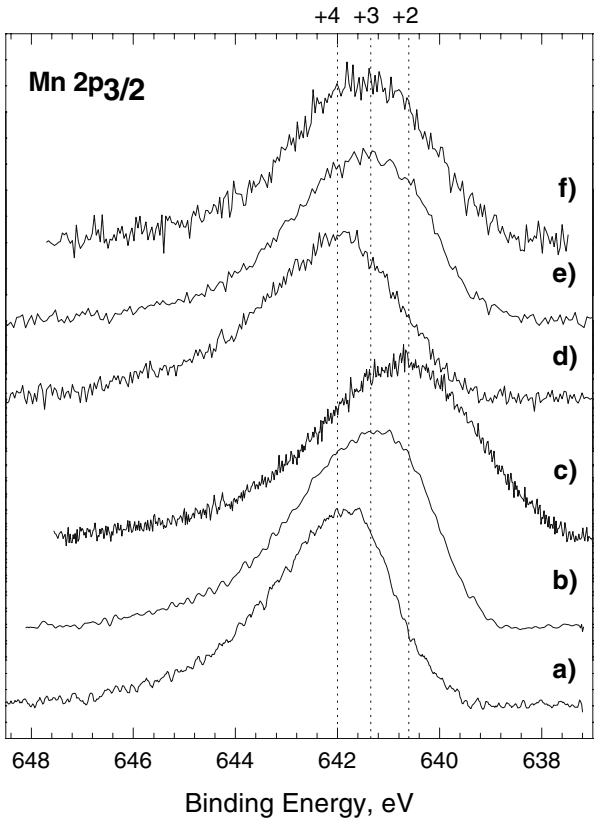

Figure 4. XPS spectra of Mn 2p in: (a) MnO_2; (b) Mn_2O_3 ; (c) MnO; (d) fresh $LaMnO_3$ perovskite calcined at 700 °C for 12.5 h; (e) the same catalyst after 20 h on stream; (f) the same catalyst after aging at 1000 °C for 24 h.

BE value reflects the allotropic transformations of aluminium oxide while the low FWHM value indicates that α-Al_2O_3 is the only form of aluminium oxide on the washcoat surface at 1000 °C.

As mentioned earlier, the washcoat was invisible in XPS analyses after the $LaMnO_3$ perovskite had been deposited. The Al 2p peak was observed again on the catalytic surface after 20 h on stream at 750 °C (figure 6b). Despite the poor spectrum quality associated with the low concentration of the Al segregated onto the surface, there is a distinct peak maximum near the value 74.3 eV; the FWHM value of 3.42 eV substantiates the presence of nonstoichiometric oxides Al_xO_y (BE being even higher than 75 eV). After aging, the FWHM value of the catalyst decreased to 2.35 eV. The position and shape of the peak maximum for 74.0 eV show that α-Al_2O_3 dominates in the washcoat and that some nonstoichiometric oxides (BE > 74.5 eV), as well as $LaAlO_3$ with a binding energy of Al 2p amounting to 73.1 eV, are also present there. For comparison, figure 6a shows the spectrum of an $LaAlO_3$ perovskite (obtained by calcining a mixture of aluminium and lanthanum nitrates at 1000 °C for 10 h) where the binding energy of Al 2p equalled 73.1 eV and was identical to the value reported by Chen [23] and Haack [24].

Spectra C1s consist of three components. The main component, in position 284.6 eV, comes from hydrocarbon contamination. The second one, around 288.7 eV, is typical of carbonate species (figure 7) [22]. When the catalyst is on stream, lanthanum carbonate decomposes to a considerable extent, but it is only above 1000 °C that this species occurs in trace amounts. The third form of binding is observed in the region of 286–288 eV, typical of C–O and C = O. The number of those bindings is remarkable, especially when the perovskite was calcined for 8h. This may be an indication that the 5-h calcination of the catalyst failed to provide a complete degradation of the lanthanum citrate that formed in the course of catalyst preparation. While on stream, the C–O and C = O bonds of the two catalysts disappeared.

3.3. Catalyst activity testing

The results of activity tests where 1% CH_4 in air was combusted in the presence of catalysts with active phases based on the $LaMnO_3$ or $LaCoO_3$ perovskite are depicted in figures 8a and 9a, as well as in table 3. Figures 8b and 9b show activity data (in the form of Arrhenius coordinates) recorded during catalytic com-

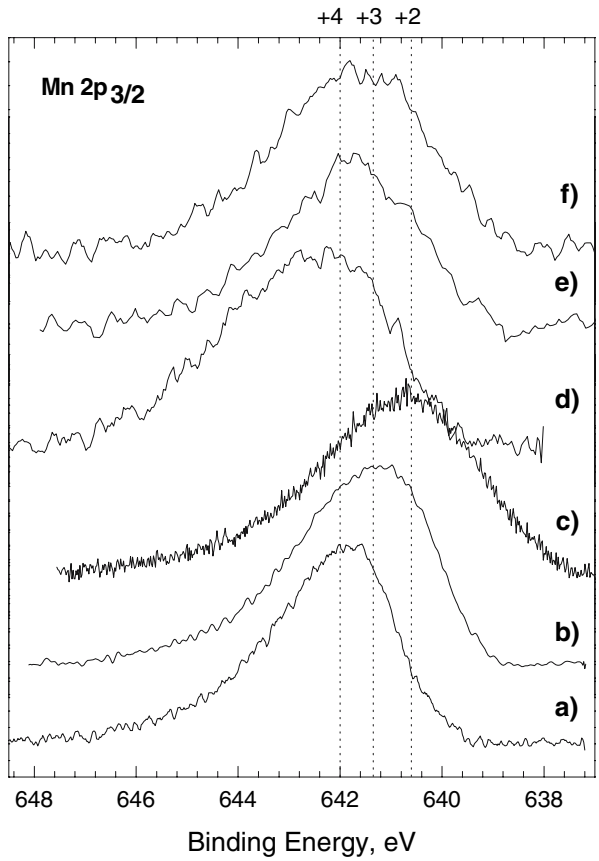

Figure 5. XPS spectra of Mn 2p in: (a) MnO_2; (b) Mn_2O_3 ; (c) MnO; (d) fresh $LaMnO_3$ perovskite calcined at 700 °C for 8 h; (e) the same catalyst after 20 h on stream; (f) the same catalyst after aging at 1000 °C for 24 h.

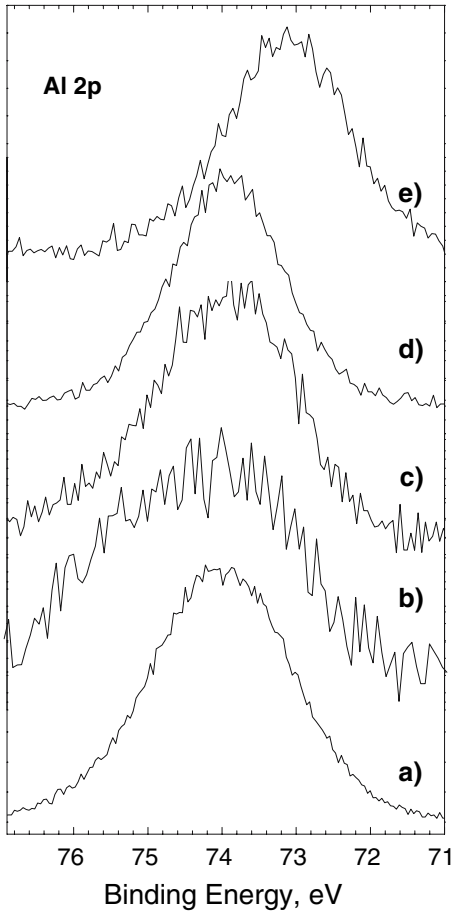

Figure 6. XPS spectra of Al 2p in: (a) γ-Al_2O_3 -washcoat after calcination at 400 °C; (b) $LaMnO_3$ catalyst after 20 h on stream; (c) $LaMnO_3$ catalyst after aging at 1000 °C for 24 h; (d) γ-Al_2O_3 washcoat after aging at 1000 °C; (e) $LaAlO_3$.

bustion of methane over $LaMnO_3$- and $LaCoO_3$-based catalysts. In the present study, apparent activation energies were determined by assuming the following: the reaction runs under isothermal ideal plug flow reactor, and is a first-order reaction relatively to methane and a zeroth-order reaction relatively to oxygen (large excess of O_2) [2,7,27–31]. The kinetic equation for methane combustion, $R = kP_{CH}4$, was substituted into the design relation for the plug-flow reactor, $F\mathrm{d}x = R\mathrm{d}w$ [27], where x is the extent of methane conversion, w is the weight of the catalyst used, and F is the molecular flow rate of CH_4. After integrating and taking logarithms of the resulting equation, we finally obtain:

$$\ln[-\ln(1-x)] = \ln\left(\frac{P_o}{F}\right) + \ln(w) + \ln(A) - \frac{E_a}{RT} \quad (1)$$

where P_o denotes initial methane partial pressure, A is the pre-exponential term of the Arrhenius equation, and E_a stands for apparent activation energy. The apparent activation energy for particular catalysts was calculated from the slopes of the plots of $\ln[-\ln(1-x)] = f(1000/T)$.

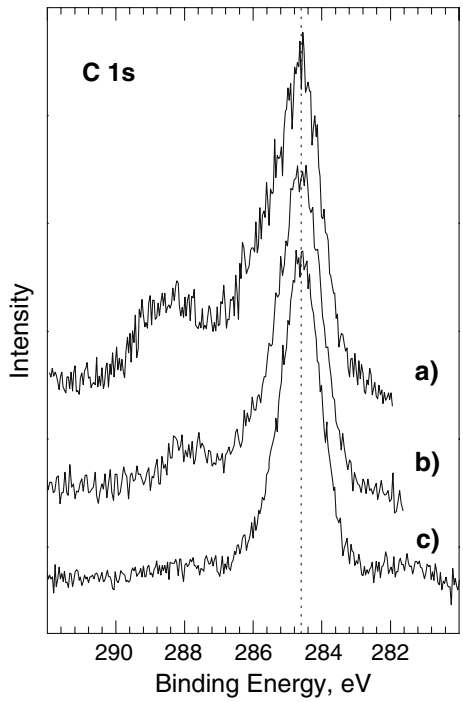

Figure 7. XPS spectra of C 1s of $LaMnO_3$ perovskite calcined at 700 °C for 12.5 h: (a) fresh; (b) after 20 h on stream; (c) after aging at 1000 °C for 24 h.

For any of the fresh monolithic $LaMnO_3$ catalysts, linear Arrhenius plots were obtained over the range of conversion between 4% and 80%. The calculated apparent activation energies are summarized in table 1. Thus, the activation energies of methane combustion over monolithic $LaMnO_3$ catalysts calcined at 700 °C for 11–12.5 h approach 73 kJ/mol; those over catalysts calcined at 700 °C for 8 h and at 750 °C for 6 h are higher, amounting to 86.3 kJ/mol and 87.3 kJ/mol, respectively. Similar activation energy values have been reported for fresh supported $LaMnO_3$ catalysts, and when such catalysts were calcined at 800 °C for 3 h, they vary between 76.3 and 92.0 kJ/mol [2,6,8,30–32]. After aging at 920 °C for 24 h, the activation energy for the monolithic $LaMnO_3$ catalyst (calcined at 700 °C for 12.5 h) does not change, as suggested by the presence of active sites of the same chemical nature on the catalyst surface. When the same catalyst has been aged at 1000 °C, activation energy increases to 107 kJ/mol, which is an indication that better crystallized $LaMnO_3$ active sites are present on its surface. Cimino et al. [6] have found that, after aging at 900 °C for 2 h, the apparent activation energy for an $LaMnO_3$ catalyst on a monolithic cordierite has increased from 76.3 kJ/mol to 80 kJ/mol; after aging at 1100 °C, activation energy has increased to 96.7 kJ/mol. The literature includes references to a rise in apparent activation energy as high as to 146.6–156.7 kJ/mol [6,31], obtained for the same type of catalysts with other methods of preparation after aging at 1100 °C. The activation energy determined for the

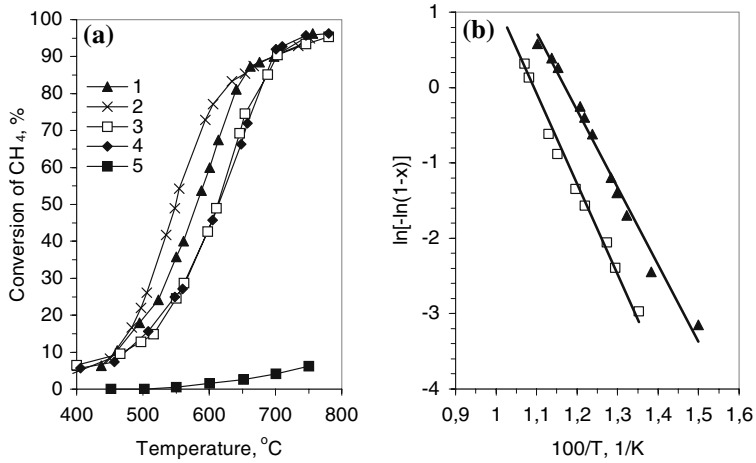

Figure 8. Methane conversion as a function of temperature (a) and corresponding Arrhenius plots (b) for fresh $LaMnO_3$ and $LaCoO_3$ catalysts calcined at 750 °C for 6 h. Catalysts: (1) 11.5% $LaMnO_3$; (2) 17.8% $LaMnO_3$; (3) 14% $LaCoO_3$; (4) 22.7% $LaCoO_3$; (5) empty reactor.

$LaCoO_3$ catalyst is by approximately 10 kJ/mol higher (97.1 kJ/mol) than that for the $LaMnO_3$ catalyst prepared with the same method.

The activities of monolithic catalysts with active phases based on the $LaMnO_3$ perovskites in the combustion of 1 vol.% methane in air are plotted in figures 8a and 9a, and summarized in table 3. Table 3 shows the values of T_{10}, T_{50} and T_{90} (the temperature at which methane conversion equals 10%, 50% and 90%, respectively) for the catalysts with $LaMnO_3$ active layers, where the perovskite was prepared at 700 °C and varying calcination time (for fresh catalysts and catalysts after 6 h on stream at 750 °C). As it may be inferred from these data, the extension of the calcination time for the perovskite from 11 h to 12.5 h was without any effect on catalytic activity, despite the decrease in the SSA of the perovskite powders with the increase in calcination time (12.89 m^2/g and 9.45, respectively). The SSA of the perovskite powder calcined for 8 h is slightly higher (13.74 m^2/g) and correlates well with that estimated by Alifanti et al. for the $LaMnO_3$ perovskite obtained by the citrate method and calcined for 5 h at 700 °C (16.5 m^2/g) [14]. However, the T_{10} and T_{50} temperatures achieved over this catalyst were higher than those obtained over the catalysts calcined for 11 and 12.5 h. The value of T_{90} was the same for all catalysts, amounting to 650 °C. The lower catalytic activity after 8-h calcination at 700 °C may be due to the incomplete formation of the $LaMnO_3$ perovskite and to the presence of a certain amount of La_2O_3 detected on the catalyst surface by XRD and XPS analyses (figures 1a and 3b). In the course of further preparation, La_2O_3 can react with citric acid to form lanthanum citrate. XPS analyses have revealed products of incomplete degradation of this species at 500 °C (during calcination of the catalyst), which may also reduce catalytic activity. What is more, XPS analyses show that the Mn:La ratio on the surface of the catalyst calcined at 700 °C for 8 h is much lower compared with the catalyst calcined for 12.5 h (0.48 and 1.8, respectively). After approximately 6 h on stream during methane combustion (at 750 °C), the activity of the catalyst increased to approach that of the catalysts with $LaMnO_3$ perovskite calcined at 700 °C for 12.5 h (table 3). XPS analyses have revealed an increase in the Mn:La ratio, which is indicative of a progressing segregation of Mn to the catalyst surface. After 20 h on stream at 750 °C, the Mn:La ratio on the surface of the active layer rose from 0.48 to 0.61. The segregation of Mn to the catalyst surface cannot fully explain why the activity of the catalyst which has been calcined for 8 h is higher, because the Mn:La ratio was still lower as compared to the catalyst with a perovskite calcined for 12.5 h (2.5 after 20 h on stream). Thus, the higher activity of the catalyst that has been calcined for 8 h seems to be linked with a higher Mn^{+4} amount on its surface as compared to the catalyst calcined for 12.5 h (figures 4, 5). And this is parallelled by a greater number of lattice defects. Structural defects determine a different oxygen mobility in the perovskite lattice, and thus influence the course of the methane oxidation reaction [28,29].

In the range of elevated temperatures (above 600 °C), there appears a concurrence of catalytic and homogeneous oxidation of methane. However, our research onto methane combustion in the empty quartz reactor has shown that the role of the homogeneous oxidation reaction at temperatures of catalytic oxidation of methane over perovskite catalysts is negligible because at 750 °C only 6.2% of methane is converted and no carbon oxide is formed in this reaction (figures 8a and 9a).

The increase in the temperature of $LaMnO_3$ calcination from 700 °C to 750 °C, with a concomitant shortening of the calcination time from 8 to 6 h, brought about a reduction in the SSA of the perowskite powders from 13.74 m^2/g to 8.58 m^2/g (table 1). Thus, even

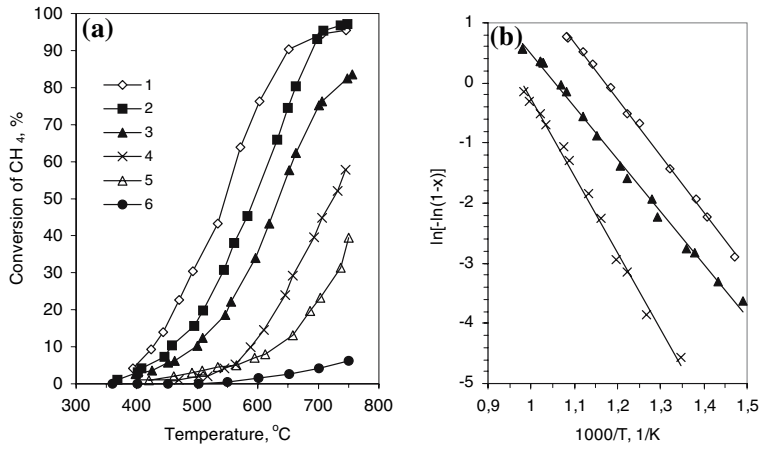

Figure 9. Methane conversion as a function of temperature (a) and corresponding Arrhenius plots (b) for $LaMnO_3$ catalysts calcined at 700 °C for 12.5 h: (1) fresh; (2) after 20 h on stream; (3) after 24 h of aging at 920 °C; (4) after 24 h of aging at 1000 °C; (5) monolith with washcoat; (6) empty reactor.

though a greater amount of the active layer had been deposited, a 90% conversion of methane over the catalyst was attained at a temperature by 50 ° higher than over the catalyst with a perovskite calcined at 700 °C for 8 h (table 3).

The results of methane combustion over the $LaMnO_3$ catalyst were compared with those obtained over the $LaCoO_3$ catalyst (figure 8a). The physicochemical characterization of the $LaCoO_3$ catalyst based on XRD, XPS and SEM data, as well as the method of catalyst preparation, has been included in previous papers [33, 34]. Both catalysts were obtained by thermal decomposition of appropriate aqueous solutions of nitrates at 750 °C for 6 h. Comparisons show that the catalyst with the $LaMnO_3$ active layer displays a distinctly higher activity. This should be attributed to the noticeably higher SSA (8.56 m^2/g) of the $LaMnO_3$ than of the $LaCoO_3$ perovskite (5.69 m^2/g). From the SEM micrographs it is seen that the crystallites occurring on the surface of the $LaCoO_3$ catalyst are much greater (from 7.2 μm to 22 μm) than the ones on the surface of the $LaMnO_3$ catalyst (from 4 μm to 8 μm) and that the surface of the $LaCoO_3$ catalyst displays far more cracks than the surface of the $LaMnO_3$ catalyst (figure 10).

In the presence of $LaMnO_3$ catalysts, the conversion of methane depended on the amount of the active layer. Over monolithic catalysts with an 11.5% and a 17.8% content of $LaMnO_3$ (figure 8a), methane combustion initiated at 460 °C (T_{10}) to yield a 90% conversion at 700 °C (T_{90}). Over the temperature range of 460–700 °C, methane conversion increased with the amount of the active layer in the catalyst. With an 11.5% $LaMnO_3$ content, 50% conversion of methane was attained at 580 °C. A 17.8% content of the active layer yielded 50% methane conversion at 550 °C. The amount of the active layer was without any effect on methane conversion in the presence of $LaCoO_3$ catalysts. The conversion of methane was the same over the entire

Table 3
Temperatures of light-off (T_{10}), 50% conversion (T_{50}) and 90% conversion (T_{90}) of methane over monolith supported $LaMnO_3$ perovskite catalysts

Composition of active phase	Catalytic activity in terms of conversion temperature (°C)		
	T_{10}	T_{50}	T_{90}
$LaMnO_3$ calcination at 700 °C for 8 h			
Fresh state	455	566	650
After 6 h on stream (750 °C)	450	550	650
$LaMnO_3$ calcination at 700 °C for 11 h			
Fresh state	430	550	650
After 6 h on stream (750 °C)	450	556	655
$LaMnO_3$ calcination at 700 °C for 12.5 h			
Fresh state	430	548	650
After 6 h on stream (750 °C)	453	565	690
17.8% $LaMnO_3$ calcination at 750 °C for 6 h			
Fresh state	460	550	700

range of the investigated temperatures, regardless of whether the active layer content amounted to 14 wt.% or 22.7 wt.%. In the presence of any of the monolithic $LaMnO_3$ perovskite-based catalysts under test, no CO or NO_x was detected in the gases from methane combustion. When methane was combusted over the monolithic $LaCoO_3$ perovskite-based catalyst at 620–650 °C, the reaction gases contained CO (13 ppm). Following a rise in temperature to 700 °C, CO concentration dropped to 2 ppm. No NO_x was detected in the reaction gas.

Aging of the catalyst with an $LaMnO_3$ active layer (calcination at 700 °C for 12.5 h), carried out at 920 °C for 24 h, accounted for a reduction in the conversion of methane over the whole range of the investigated temperatures. At 746 °C, methane conversion dropped from 95.5% to 82.5%. When the temperature of aging was raised to 1000 °C, this was concomitant with a considerable deterioration of the combustion effect. Methane conversion at 745 °C was as low as 57.8% (figure 9a). However, as it can be seen in figure 9a, the activity of the catalyst after aging at 1000 °C is still higher than that of the Al_2O_3 -washcoated monolithic support. This pattern of behaviour is attributable to the sintering of the perovskite and decrease in SSA from 9.45 m^2/g to 1.0 m^2/g, as well as to the change in the composition of the catalyst surface. As it may be inferred from XPS analysis, the aging of the catalyst brought about a decrease in the Mn:La ratio (from 1.8 to 1.7) and an increase in the ratios of C:La (from 3.9 to 11.3) and Al:La (from 0 to 1.5).

3.4. *Catalyst resistance to thermal shock*

With monolithic catalysts used in methane combustion, it is not only catalytic activity but also a good adhesion of the active layer and washcoat to the support that matters. The alternate cycles of heating up to 1000 °C and cooling down to 20 °C can cause cracking of the washcoat and active layer due to the difference in thermal expansion between them, thus leading to their drop-off. This, in turn, reduces the amount of the active layer and, consequently, the activity of the catalyst.

The plots of figure 11 show the relative weight loss for the catalysts with $LaMnO_3$ or $LaCoO_3$ active layers (calcined at 750 °C for 6 h) with respect to the number of heating and cooling cycles. The relative weight loss was calculated as the ratio of the decrease in the weight of the catalyst to the initial total weight of the monolith. Increasing the amount of the active layers brings about a reduction in their adhesion to the support (figure 11). As shown by these plots, the $LaCoO_3$-based catalyst displays a higher resistance to quick temperature variations. After 3900 cycles of thermal shocks, weight loss in the catalyst with a 22.7% $LaCoO_3$ content amounted to 2.5 wt.% while that in the catalyst with a 17.8% $LaMnO_3$ content equalled 6.4 wt.%. The extension of the time of perovskite calcination at 700 °C from 8 h to 12.5 h reduced the thermal resistance of the monolithic catalyst. Following 4000 heating and cooling cycles, relative weight loss amounted to 0.8 wt.% and 3.8 wt.%, respectively.

4. Conclusions

The activity and thermal resistance of the metallic monolithic supported $LaMnO_3$ catalyst depend on the temperature, time of perovskite calcination and the amount of the active layer.

The chemical compositions of the surfaces of $LaMnO_3$ catalysts determined by the XPS method differ remarkably from those obtained by stoichiometry. What deserves particular attention is the Mn-enrichment (Mn:La = 1.8) of the surface of the catalyst calcined for 12.5 h, in contrast to the surface of the catalyst calcined for 8 h, which is poor in Mn (Mn:La = 0.48). This

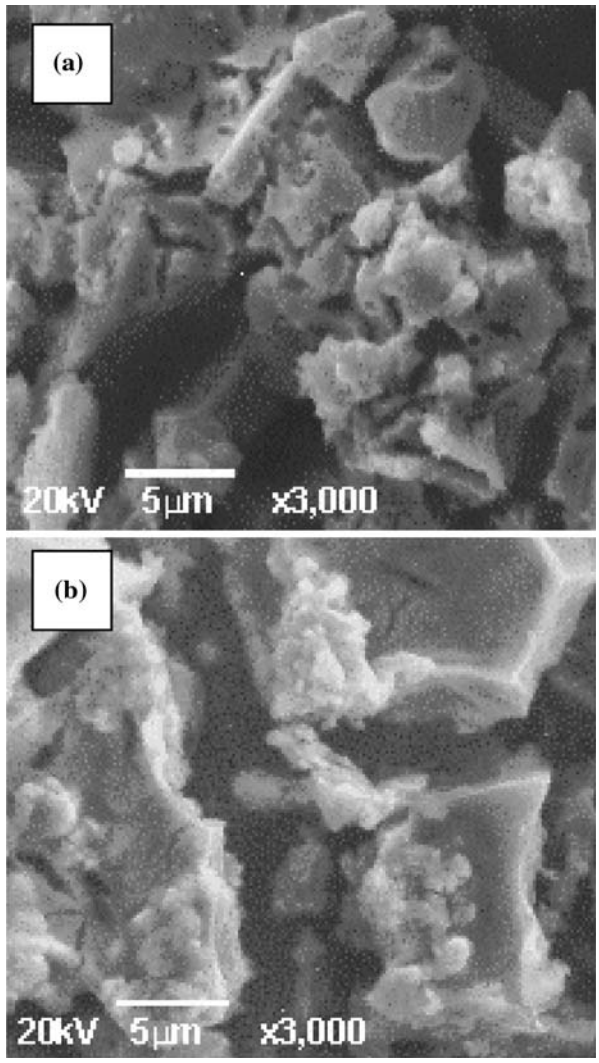

Figure 10. SEM images of the surfaces of $LaMnO_3$ (a) and $LaCoO_3$ (b) perovskite-based monolithic catalysts. The perovskite was calcined at 750 °C for 6 h.

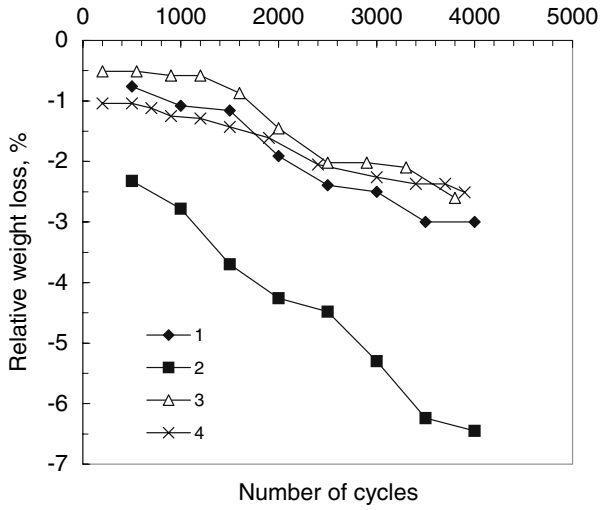

Figure 11. Resistance of catalysts to thermal shocks: (1) 11.5% $LaMnO_3$; (2) 17.8% $LaMnO_3$; (3) 14% $LaCoO_3$; (4) 22.7% $LaCoO_3$.

reverse proportion is very likely to be responsible for the reduced activity of the fresh catalyst which has been calcined for a shorter time, irrespective of whether its structure was or was not a fully developed perovskite.

After only several hours on stream, the catalyst with a perovskite calcined for 8 h showed a slightly higher activity than did the catalyst with a perovskite calcined for 12.5 h. This is due to the segregation of Mn to the catalyst surface. The rise in catalytic activity was also contributed by the greater amount of Mn^{+4} than Mn^{+3} ions determining the occurrence of structural defects.

Aging of the catalyst with an $LaMnO_3$ active layer at 920 °C or 1000 °C for 24 h reduces its activity. The drop in catalytic activity is due to the decrease in the SSA of the perovskite and to the change in the composition of the catalyst surface, where the content of aluminium and carbon increases notably while the Mn:La ratio decreases. The main component of segregated aluminium is α-Al_2O_3, although some nonstoichiometric aluminas, as well as $LaAlO_3$, are also present there.

Methane conversion is greater over the metallic monolithic supported $LaMnO_3$ catalysts than $LaCoO_3$ catalysts, but the latter display a higher resistance to thermal shocks.

References

[1] C. Batiot-Dupeyrat, F. Martinez-Ortega, M. Ganne and J.M. Tatibouet, Appl. Catal. A: General 206 (2001) 205.
[2] P. Salomonsson, T. Griffin and B. Kasemo, Appl. Catal. A: General 104 (1993) 175.
[3] D. Ferri and L. Forni, Appl. Catal. B: Environ. 16 (1998) 119.
[4] I. Rossetti and L. Forni, Appl. Catal. B: Environ. 33 (2001) 345.
[5] G. Xiong, Z.L. Zhi and X. Yang, J. Mater. Sci. Lett. 16 (1997) 1064.
[6] S. Cimino, R. Pirone and G. Russo, Ind. Eng. Chem. Res. 40 (2001) 80.
[7] J.G. McCarty and H. Wise, Catal. Today 8 (1990) 231.
[8] S. Cimino, R. Pirone and L. Lisi, Appl. Catal. B: Environ. 35 (2002) 243.
[9] S. Cimino, A. Benedetto, R. Pirone and G. Russo, Catal. Today 69 (2001) 95.
[10] A. Gonzalez, E. Martinez, A.B. Porter and V.C. Corberan, Catal. Today 33 (1997) 361.
[11] P. Ciambelli, S. Cimno, S. Rossi, L. Lisi, G. Minelli, P. Porta and G. Russo, Appl. Catal. B: Environ. 29 (2001) 239.
[12] R. Leanza, I. Rossetti, L. Fabbrini, C. Oliva and L. Forni, Appl. Catal. B: Environ. 28 (2000) 55.
[13] P. Ciambelli, S. Cimino, L. Lisi, M. Faticanti, G. Minelli, I. Pettiti and P. Porta, Appl. Catal. B: Environ. 33 (2001) 193.
[14] M. Alifanti, J. Kirchnerova and B. Delmon, Appl. Catal. A: General 245 (2003) 231.
[15] T.A. Nijhuis, A.E.W. Beers, T. Vergunst, I. Hoek, F. Kapteijn and J.A. Moulijn, Catal. Rev. 43 (2001) 345.
[16] L.A. Isupova, V.A. Sadykov, S.F. Tikhov and O.N. Kimkhai, Catal. Today 27 (1996) 249.
[17] B. Biasi, Johnson Matthey Cogeneration 21 (1984).
[18] W. Jinshu, , J. Alloys Compd. 339 (2002) 293.
[19] J.W. Murray, J.G. Dillard, R. Giovanoli, H. Moers and W. Stumm, Geochim. Cosmochim. Acta 49 (1985) 463.
[20] H.W. Nesbitt and D. Banerjee, Am. Mineralogist 83 (1998) 305.
[21] S. Ponce, M.A. Pena and J.L.G. Fierro, Appl. Catal. B: Environ. 24 (2000) 193.
[22] F.A. Cotton and G. Wilkinson Advanced Inorganic Chemistry (5th edition), (Wiley, New York, 1455p).
[23] X. Chen, Y. Liu, G. Niu, Z. Yang, M. Bian and A. He, App. Catal. A: General 205 (2001) 159.
[24] L.P. Haack, J.E. De Vries, K. Otto and M.S. Chattha, Appl. Catal. A: General 82 (1992) 199.
[25] L.P. Haack, C.R. Peters, J.E. De Vries and K. Otto, Appl. Catal. A: General 87 (1993) 105.
[26] R.C. Ropp and B. Carroll, J. Am. Ceram. Soc. 63 (1980) 417.
[27] V.C. Belessi, A.K. Ladavos and P.J. Pomonis, Appl. Catal. B: Environ. 31 (2001) 183.
[28] G. Saracco, F. Geobaldo and G. Baldi, Appl. Catal. B: Environ. 20 (1999) 277.
[29] S. Cimino, L. Lisi, S. Rossi, M. Faticanti and P. Porta, Appl. Catal. B: Environ. 43 (2003) 397.
[30] S. Cimino, A. Benedetto, R. Pirone and G. Russo, Catal. Today 83 (2003) 33.
[31] L.A. Isupova, G.M. Alikina, S.V. Tsybulya, A.N. Salanov, N.N. Boldyreva, E.S. Rusina and I.A. Ovsyannikova, , Catal. Today 75 (2002) 305.
[32] H. Arai and M. Machida, Catal. Today 10 (1991) 81.
[33] B. Kucharczyk and W. Tylus, Catal. Today 90 (2004) 121.
[34] B. Kucharczyk, Pol. J. Appl. Chem. 4 (2003) 263.
[35] T. Ranganathan, B.E. MacKean and A. Muan, J. Am. Ceram. Soc. 45((6) (1962) 279.
[36] S.J. Cho, Y.S. Seo, K.S. Song, N.J. Jeong and S.K. Kang, Appl. Catal. B: Environ. 30 (2001) 351.